

PHYS4420 Assignment: Analysis of x-ray sources within the ω -Centauri globular cluster

Joseph Hocking
22876965@student.uwa.edu.au
(Dated: October 5, 2023)

A data analysis of Chandra X-Ray observation of the ω -Centauri globular cluster, ObsID 13726 and 13727, was replicated. The original study by S. Henleywillis et al. found 233 sources, and performed spectral fitting upon 14 of the brightest known members of the cluster. Of the 14, 13 were reidentified here, and spectral fitting was repeated. This fitting found somewhat similar parameters to the original study. Additionally, the parameters, although varying, are found to still be in support of some of the major conclusions of this study, namely, the identification of a CH star as a symbiotic star, and the large proportion of high n_H CVs present in the source list, which may be due to the presence of magnetic CVs distorting the statistics of the brightest CVs.

I. INTRODUCTION

Globular clusters are broadly spherical group of stars on the order of $\sim 10^5 - 10^6$ objects. The globular cluster NGC 5139, more commonly referred to as ω -Centauri (from here on ω Cen) is a well known historical example of a globular cluster. It was first identified by Greek astronomers, who in the 2nd century AD wrongly classified it as a star. It wasn't until Edmond Halley in 1677, taking advantage of the recent invention of the telescope, discovered that it was in fact a non-stellar object, however it took a further 150 years before James Dunlop classified it as a globular cluster. It is unique in that it is the largest globular cluster known within the Milky Way, with a radius of 86 ± 6 ly and an estimated mass of $(4.05 \pm 0.1) \times 10^6 M_\odot$, which, along with other evidence for an intermediate mass black hole in its core, leads some to argue that it may in fact be a remnant of a dwarf galaxy, swallowed by the much larger Milky Way.

The main mechanism of internal cluster dynamical evolution is due to gravitational interaction between bodies. Statistically, one may derive an approximate rule for the *relaxation time* of a globular cluster as follows:

$$t_{\text{relax}} \approx \frac{0.1N}{\log N} t_{\text{cross}} \quad (1)$$

Where N is the number of stars in the cluster, and t_{cross} is the crossing time of stars within the cluster. For the ω Cen cluster, the half mass relaxation time has been found to be relatively long, at $t_{\text{relax}} \approx 10$ Gyr. This is significant as the cluster has an estimated age of ~ 12 Gyr, thus many of the dynamics within the clusters are similar to those that would occur just after formation. One may observe the effect of this relaxation time by examining the radial distribution (or rather independence) of mass-light ratio, that is, there is broadly

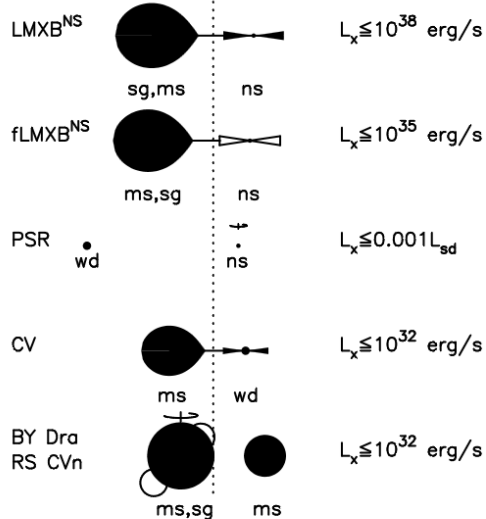


FIG. 1: A description of the potential x-ray sources within the globular clusters[1]

an even distribution of high and low mass stars. Whereas in clusters that have evolved over several relation times, the high mass stars tend to migrate towards the center of the cluster.

Another important concept to consider is the effective *negative heat capacity* of a cluster. This is a by-product of the virial theorem within a self gravitating system. Conceptually, as a body in orbit loses energy, its orbit becomes tighter, and thus the body's speed will increase (making it "hotter"). Additionally, just as in thermodynamical systems, weak gravitational interactions between stars begins to establish an equipartition of kinetic energy. This will ultimately mean stars of higher mass will slow down as they transfer speed to stars of lower mass. Thus a segregation is formed of high mass stars towards the core of the cluster and low mass towards the outside. Because of the negative heat capacity of the cluster, it's core will become denser and denser as time goes on, and relatively quickly resulting in *core collapse*. An easy analogy can be made to the structure of a star, which would undergo gravitational collapse if it were not held at equilibrium by the radiation pressure from nuclear fusion. In the case of globular clusters, the bound energy of binary star systems provide the necessary energy to keep the cluster in equilibrium. When a binary system interacts with outside binaries, there is a chance for one object in the binary to lose energy to the outside object, which through it's negative heat capacity will speed the binary system up, staving off core collapse¹. This mechanism is able to extend the time before core collapse to $\sim 10t_{relax}$. It is also interesting to note that observations have showing that insufficient numbers of binaries could be formed through encounters, given the known density of globular cluster cores, and so the majority of these are likely to be primordial binaries (or systems that *formed* as binaries).

We can split x-ray sources in general into two categories: luminous and low-luminosity. Of the luminous sources with globular cluster, it is considered widely that they are all composed of binary systems of the type shown in Figure 1, and the CVs and CH (possible symbiotic) sources described in this analysis. Additionally the vast majority of low luminosity sources are of these same type or at the very least evolved from binary systems, however the red giant branch and sub giant branch stars (also identified in this analysis) are coronal sources

¹ In fact, a single standard mass binary system of two $0.7M_\odot$ stars are able to contain more binding energy than the entire cluster they are contained within

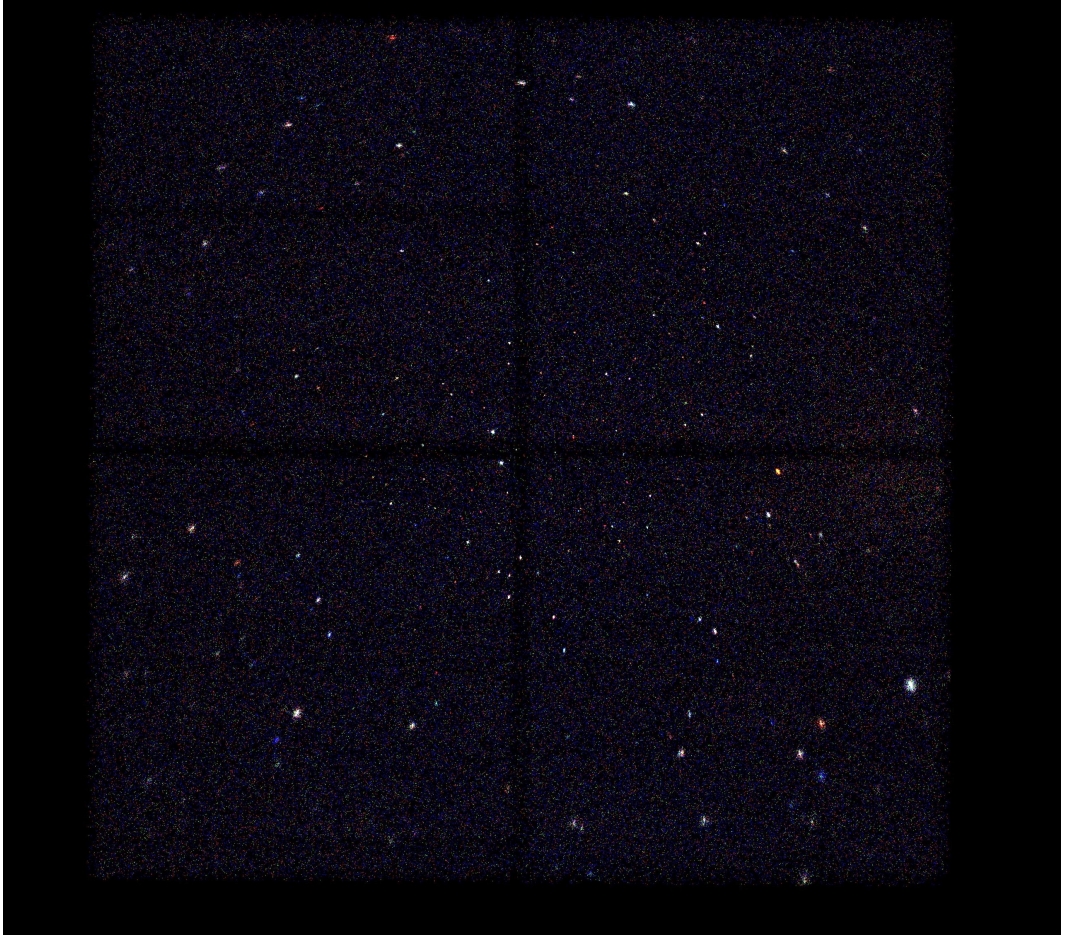


FIG. 2: True color image of the ω Cen cluster as imaged by the ACIS-I CCD's from the merged observation files. This is composed of 3 energy bands, the soft x-ray (0.2-1.5 keV) is in red, the mid x-ray (1.5-2.5 keV) is in green, and the hard x-ray (2.5-8 keV) is in blue.

The exposed image covers approximately 16.9x16.9 arcmin, with a resolution of 0.49 arcsec/pixel. The four quadrants of the image are the 4 CCDs of the instrument, with each being 1024x1024 pixels, giving a total of 2048x2048 pixels for the image.

likely from single stars. Given the relation to high luminosity x-ray sources and binaries, and given the importance of binary systems to the stability of globular clusters, studying x-ray sources within globular clusters is crucial to understanding cluster dynamics as a whole.

The remainder of this report will be split up into 2 main sections: 1) Methodology and 2) Results. In the methodology section, there will be description of the observations and data processing pipeline, the source identification process, and the spectral extraction and fitting. The results section will be a discussion of the parameter estimation produced by the spectral fitting, and an interpretation of the values based off of known source identification.

II. METHODOLOGY

This analysis examined the same two datasets used by Henley-Wellis et. al. These were long-exposure time observations, one 173.7ks (ObsID 13726) and the other 48.5ks (ObsID

13727), of the ω -Centauri globular cluster made with the *Chandra X-ray Observatory's* ACIS-I sensor. These observations, made in 2012, were targeted towards the detection of faint sources within the cluster, with more details on the set-up of the telescope in citeHenleyWellis2018. The processing and analysis (performed using the tools CIAO and XSPEC) described herein will follow a very similar procedure as that used by Henley-Wellis et. al. To begin with, the two observations were reprocessed using CHANDRA_REPRO as recommended by the documentation accompanying CIAO. This tool accepts in the level 1 events files (that is, the raw data) and uses the most up-to-date calibration data appropriate for the observation to generate new level 2 event files. Before source-detection was performed, the reprocessed data files were then combined using the MERGE_OBS tool, which also generated fluxed images, exposure maps, field-of-view files, and a merged point-spread function map (PSF). Henley-Wellis et al. generated these PSF maps outside of MERGE_OBS, however, as the specified parameters are identical, this should not change the data files. These merged observations were limited to 0.5-4.5keV to reduce the background sources that could potentially be detected. The PSF maps were generated at 1.9keV and were merged by weighting the respective PSF maps for each observation by the exposure time. Additionally, an encircled counts fraction of 0.5 was selected. This was chosen to match the processing performed by Henley-Wellis et. al, who in turn found this value to give optimal source distinction.

The source detection was performed on the merged observation using the WAVDETECT algorithm. Within CIAO, this works via a two step process: firstly, it performs a wavelet transform by correlating it with wavelet functions of the wavelet-scale sizes, and secondly a cell is generated around each source based off of the information from the wavelet transform. As per Henley-Wellis et al., wavelet scales of 1, 2, 4, and 8 were used, along with a significance threshold of $1e - 06$ (this is the significance required for classifying a pixel as belonging to a source). In total, 240 sources were identified, many of which are likely background background sources.

To simplify the analysis, only the 14 of brightest sources (as in table 3 of Ref citeHenleyWellis2018) detected underwent spectral fitting. Not only did these sources benefit from having the highest counts, thus improving the fitting results, but also have previously been shown to be cluster members by Henley-Wellis et. al. To identify which of the detected sources corresponded with those described, DMCOPY was used to extract all detected sources above 70 counts in the 0.5-4.5keV band². Of the 14 sources sought after, 13 were detected, with the final source being 73a, which was the dimmest of the sources (the full source identification list is given in **TODO**). Regardless this was more than sufficient to continue on to the spectrum extraction of the sources.

Spectrum extraction was performed on each individual observation (ie. the level 2 event files as produced by CHANDRA_REPRO) for the source regions identified. To do so, the .FITS region files outputted by WAVDETECT were converted into ASCII.REG files using DMMAKEREG. These were then used to create a list (as a .LIS file) of virtual files, which each virtual file corresponding to a source region within the observation. Then the CIAO tool SPECEXTRACT was run on this list, with a few important parameters, namely the WEIGHT=NO essentially telling SPECEXTRACT to treat the sources as point sources and to not spatially weight the auxiliary response files (ARF), and CORRECTPSF=YES which tells the tool to apply a point-source aperture correction to the *unweighted* ARF. This generated 26 spectra, 1 spectra for each source and each observation, along with additional response files. The spectra for each source from the two observations were then summed using the COMBINE_SPECTRA tool.

² Henley-Wellis et. al. used counts in the 0.5-6keV, this is likely with source 14 (73a) was missed

The script used to fit the spectra within XSPEC is shown in Appendix **TODO**. Utilizing *C-statistics* to account for the low count numbers³. A TBABS*VMEKAL model was used to fit to the data. TBABS is the Tuebingen-Boulder interstellar medium absorption model derived from Ref citeTBABS references. It accepts only the single parameter, n_H , the equivalent hydrogen column. VMEKAL is a model for the emission from a hot, diffuse gas, including the emission lines from several elements. It accepts 19 parameters in total, with the free parameters being the temperature and a normalisation. The other parameters were the H density (fixed to $3 \times 10^{21} \text{cm}^{-2}$)⁴, the abundances for the elements, (which were set to Solar abundance, excluding Fe, which was set to 0.03 Solar as per the [Fe/H]=-1.5 listed in citeHenleyWellis2018), the redshift (set to 0), and a switch parameter to tell the model to use emission lines from the AtomDB data. The equivalent hydrogen column for the TBABS model had a lower bound of $9 \times 10^{20} \text{cm}^{-2}$, and was occasionally fixed at this value as shown in Table **TODO**. After fitting, 90% confidence intervals for the free parameters were calculated using XSPEC's ERROR function, and a luminosity value in the 0.5-6keV band was calculated for each source using LUMIN⁵.

III. RESULTS AND DISCUSSION

The fitted parameters, as well as other source information is given in Table I, and 4 of the more interesting spectra are shown in Fig 5. Before examining specific sources, a few comments on the overall fitting are warranted. For the high luminosity sources, this analysis tended to underestimate when compared to the original. However, the uncertainty of the luminosities do overlap for the most part, suggesting that the difference may come down largely to statistical uncertainty. Also, for some best fit parameters (eg. source 4 temperature), the value was significantly larger than what was concluded previously. Additionally, the uncertainty on this parameter could not be calculated, as the ERROR function got stuck in an non-terminating loop. This leads to the conclusion that such parameters are unreliable and should not be used to compare previous results. Likely, the fitting was stuck inside a local minimum, however insufficient further analysis of the fitting would need to be performed to verify this.

³ This is based upon Poisson counting statistics, as opposed to the default χ^2 based upon Gaussian statistics, this gives C-statistics a distinct advantage in the low count regimes.

⁴ This was an estimation made after experimenting with the fitting parameters, it also coincides with an approximate middle value for the n_H parameter given in Ref citeHenleyWellis2018 Table 3 when excluding the high absorption sources.

⁵ This function required a non-zero redshift to be inputted, which was estimated from the distance to the globular cluster (5.2kpc) and $H_0 = 70 \text{km s}^{-1} \text{Mpc}^{-1}$, giving $z = d * H_0 / c \approx 1.2 \times 10^{-6}$

Source ID	RefHWID	Type	Position (RA[+201], DEC[-47])	Counts (0.5-4.5keV)	n_H (10^{20} cm $^{-2}$)	kT (keV)	L_x (10^{30} ergs s $^{-1}$)
1	13c	CV	(0.7172 \pm 3.7, 0.4932 \pm 2.7)	2095(2042)	12 $^{+6}_{-\infty}$ (16)	49.1 $^{+\infty}_{-29.2}$ (34)	537 $^{+21}_{-24}$ (570)
2	13a	CV	(0.7123 \pm 4.0, 0.4834 \pm 2.7)	1924(1860)	47 $^{+13}_{-7}$ (51)	13.8 $^{+8.3}_{-3.7}$ (14.4)	398 $^{+18}_{-40}$ (423)
3	94a	CH	(0.5067 \pm 32, 0.5516 \pm 27)	1018(1088)	41 $^{+8}_{-9}$ (72)	24.0 $^{+26.8}_{-10.1}$ (6.8)	368 $^{+15}_{-13}$ (466)
4	54h	CV	(0.5849 \pm 20, 0.5008 \pm 17)	387(394)	22 $^{+16}_{-10}$ (37)	61.9 $^{+\infty}_{-\infty}$ (19.2)	90 $^{+20}_{-90}$ (98)
5	41d	CV	(0.6194 \pm 14, 0.4408 \pm 9.5)	363(360)	94 $^{+27}_{-23}$ (112)	17.7 $^{+\infty}_{-9.1}$ (14.6)	117 $^{+7}_{-54}$ (117)
6	43h	CV	(0.7066 \pm 16, 0.5368 \pm 15)	223(208)	9 $^{+13}_{-\infty}$ (12)	10.8 $^{+16.2}_{-5.2}$ (6.8)	51 $^{+1}_{-15}$ (54)
7	22c	fbCV	(0.7195 \pm 11, 0.4536 \pm 7.7)	180(179)	9 $^{+6}_{-\infty}$ (11)	5.6 $^{+5.8}_{-1.9}$ (5.7)	31 $^{+3}_{-7}$ (39)
8	11b	NV371	(0.6707 \pm 13, 0.4604 \pm 11)	172(173)	9 $^{+\infty}_{-\infty}$ (9)	2.8 $^{+1.1}_{-0.9}$ (3.2)	24 $^{+1}_{-6}$ (26)
9	31a	fbCV	(0.6224 \pm 20, 0.4703 \pm 15)	120(119)	18 $^{+25}_{-\infty}$ (21)	25.3 $^{+\infty}_{-19.9}$ (22.3)	27 $^{+1}_{-27}$ (27)
10	54b	fbCV	(0.6770 \pm 28, 0.5525 \pm 37)	105(103)	137 $^{+69}_{-33}$ (196)	75.5 $^{+\infty}_{-\infty}$ (13.0)	35 $^{+35}_{-20}$ (34)
11	34b	RGB/SGB-a	(0.6560 \pm 25, 0.5147 \pm 24)	87(87)	51 $^{+36}_{-27}$ (55)	2.9 $^{+2.6}_{-1.0}$ (2.7)	16 $^{+2}_{-3}$ (17)
12	32f	RGB/SGB-a	(0.7723 \pm 37, 0.4691 \pm 26)	77(73)	9*(9*)	3.9 $^{+5.6}_{-1.1}$ (2.2)	13 $^{+1}_{-3}$ (12)
13	24c	CV	(0.6601 \pm 22, 0.5101 \pm 15)	72(71)	9*(9*)	6.4 $^{+19.2}_{-3.1}$ (5.7)	12 $^{+1}_{-3}$ (12)

TABLE I: List of X-ray sources within ω Cen. The types are as described in Ref citeHenleyWellis2018. The positions were determined by the source detection algorithm in degrees (with the listed offset +201 and -47 for right ascension and declination respectively), and the uncertainty is given in (10^{-6}) $^{\circ}$. In the remaining columns, the value determined by this analysis is given, with the value from Ref citeHenleyWellis2018 given in parentheses. The counts were determined automatically from WAVDETECT and the uncorrected counts are given from Ref citeHenleyWellis2018. A * represents that the parameter was fixed during the fit. The ∞ in the uncertainty means that either the error calculation hit the lower and upper bound for the given parameter, or that the error calculation did not terminate.

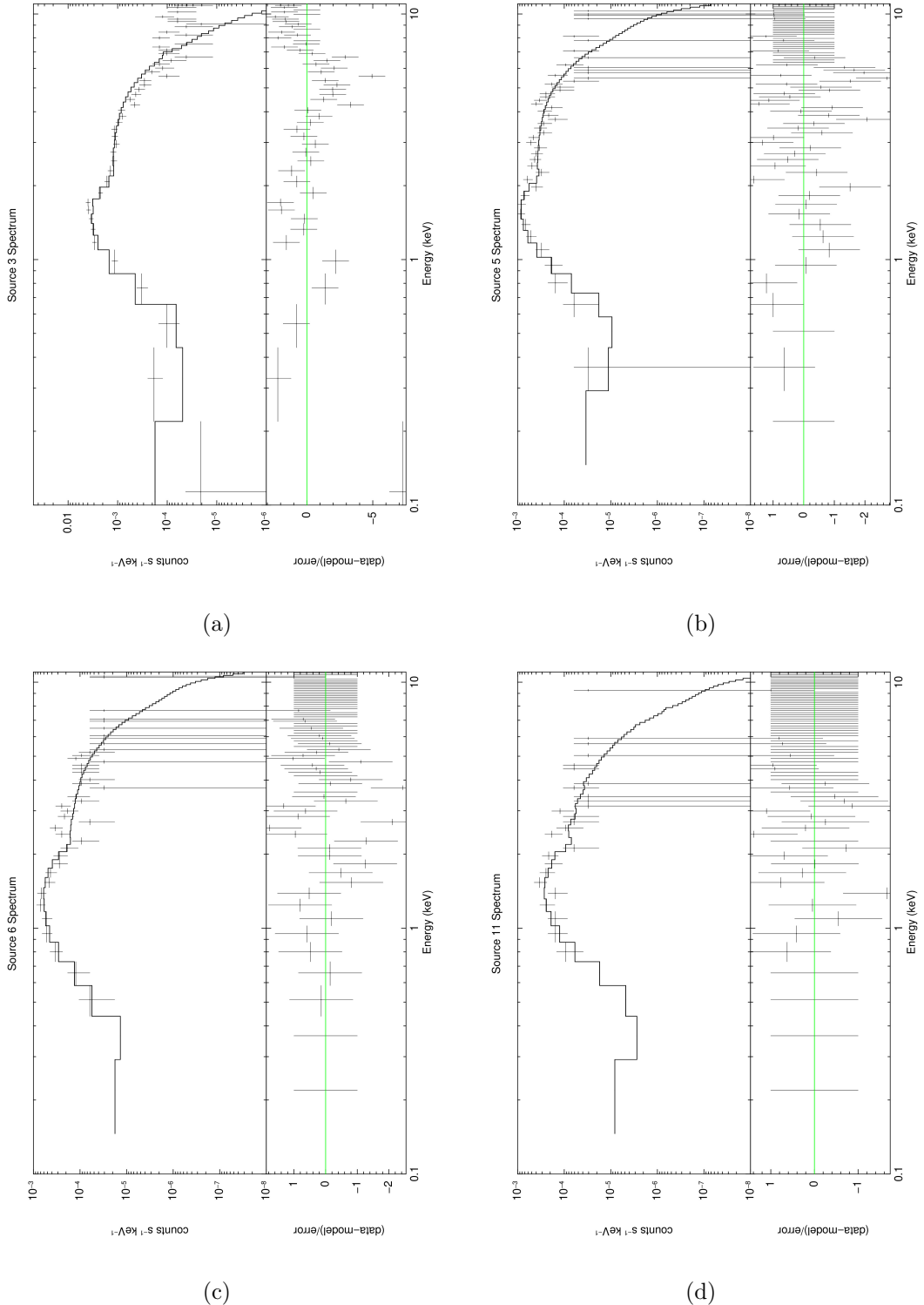


FIG. 3: A selection of fitted spectra and residuals. **(a)** is source 3, which is identified to be a CH star. **(b)** is a cataclysmic variable with high internal absorption, with **(c)** being an example of a CV with cluster average absorption. Finally **(d)** is a RGB/SGB-a star. Note that the binning is performed for plotting only and is not present during fitting.

A. Source 3: A CH star

One of the more notable conclusions from Ref citeHenleyWellis2018 is that the source 3, previously identified optically as a CH star, may be a symbiotic binary, the first such star in a globular cluster. In this analysis, the expected higher than cluster medium absorption ($n_H \approx 4 \times 10^{21} \text{ cm}^{-2}$) was replicated in the modelling. However a much higher plasma temperature ($kT \approx 25 \text{ keV}$) was observed in the fitting. With that being said, these values still fall within a reasonable range for what a symbiotic binary would be expected to have citeLuna2013. To confirm this conclusion further observations would need to be made, however. For one, we expect the hard x-ray emission to time-variable, not only this, but symbiotic stars with high energy emissions ($kT \sim 5\text{-}50 \text{ keV}$) experience the greatest variability in their UV spectrum.

B. Source 5 and 6: Cataclysmic variables

There are many CVs identified within the globular cluster. Of the 13 brightest sources listed here, 9 of them have been identified as CVs. Interestingly, though 6 of these CVs required higher than cluster average absorption to be fitted correctly (just as in Ref cite-HenleyWellis2018). In the original paper, two explanations are given for this. Firstly, if the CV's are orientated such that the binary system is ecclipsed, then high absorption is known to occur citeHeinke2005. It is very improbable that this explain all of the high n_H CVs present within this observation, simply due the statistical unlikeliness of having so many systems orientation in such a specific manner. Instead, citeHenleyWellis2018 suggest that the high absorption could be due to magnetism being present within some of the systems. These are CV systems with 'mid-strength' magnetic field, strong enough to disrupt the accretion somewhat, but not stall it entirely. It is estimated, though, that magnetic CVs only make up around 20% of all CVs, so this does not directly explain the large proportion of high n_H CVs present in this source list. However, also due to the magnetic field direct accretion flow close to radially, it is expected the magnetic CVs will exhibit a brighter x-ray emission than non-magnetic CVs citePretorius2013. This bias in the sampling of the source list could go a long way in explaining the large fraction of high n_H CVs present. Though ultimately, again, more observations will be required to confirm this explanation, potentially performing spectral fitting of a larger population of CVs with ω Cen will reveal the true proportion of the high n_H CVs present.

IV. CONCLUSION

An analysis of *Chandra* ACIS-I obervations of the globular cluster ω Cen has been replicated. Two datasets were merged and utilised, to give a total exposure time of 220ks, allowing good detection of faint sources. The 13 brightest sources were selected and indentified within the results of the original study. A spectral fitting of these sources was performed, modelling them with a composite model within XSPEC, TBABS and VMEKAL, providing insight into the internal absorption and temperature of the sources identified. For the most part, the fitting paramaters are within the 90% confidence interval given, and so match the original analysis. For the parameters that vary greatly (eg. some temperature values), it was shown that likely they are due to local minima in the fitting process, and thus may be disregarded.

The CH star, which is source 3, had similar parameters to that described originally, though with a lower n_H and higher kT . Thus, leading a similar identification of this system being a possible symbiotic star. Also replicated, was the large proportion of high n_H CVs present in the source list. This again lends further credance to the explanation given in the original paper. Overall, this replication report strongly supports these conclusions given in the study, however, with all things, further observations are required to validate these claims, namely observations within different energy bands, such as UV, and spectral fitting of fainter CVs.

- [1] F. Verbunt and W. H. G. Lewin, Globular cluster x-ray sources, in *Compact Stellar X-ray Sources*, Cambridge Astrophysics, edited by W. Lewin and M. van der Klis (Cambridge University Press, 2006) p. 341–380.

Appendix A: Spectra for all sources identified

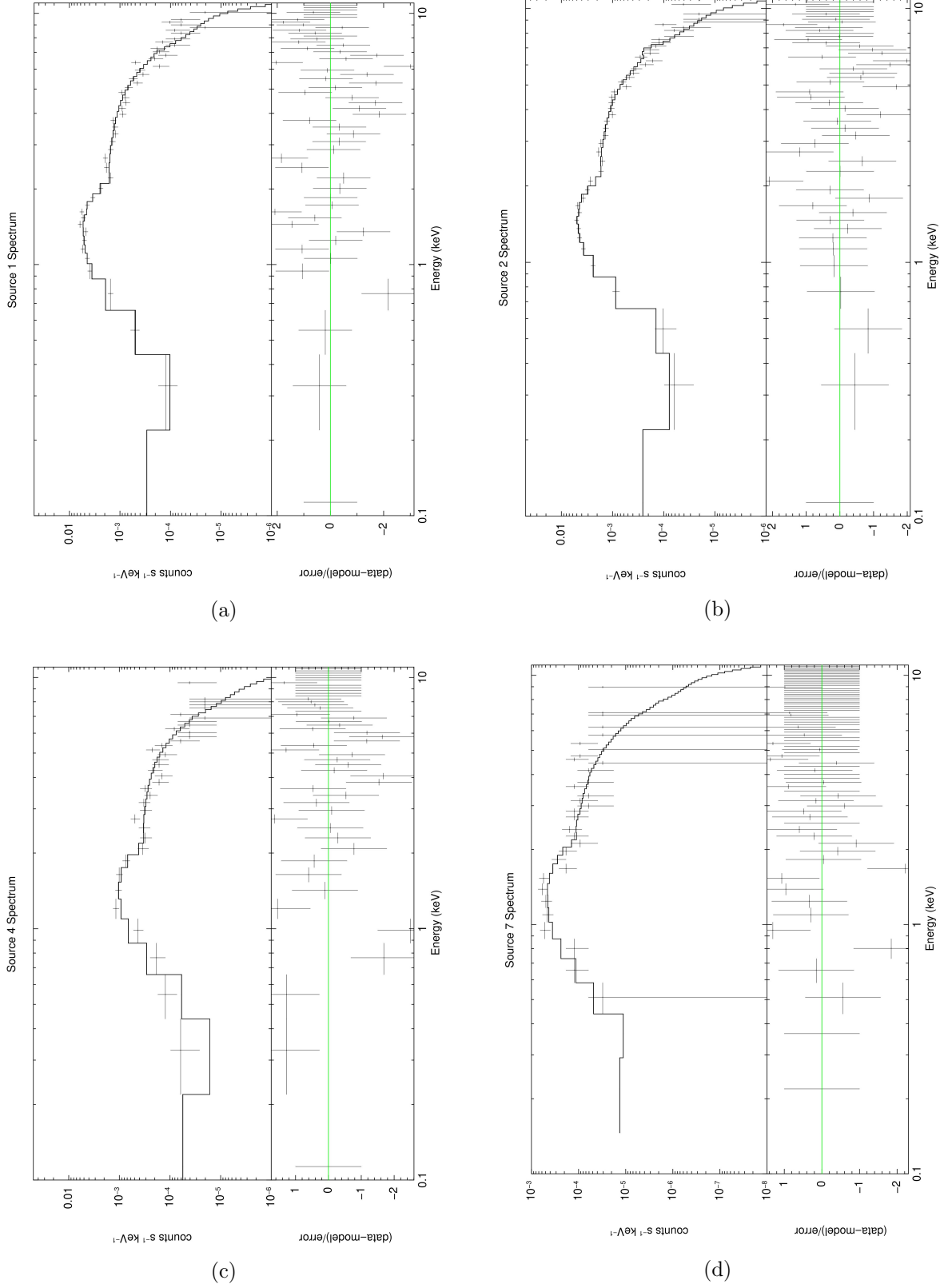


FIG. 4

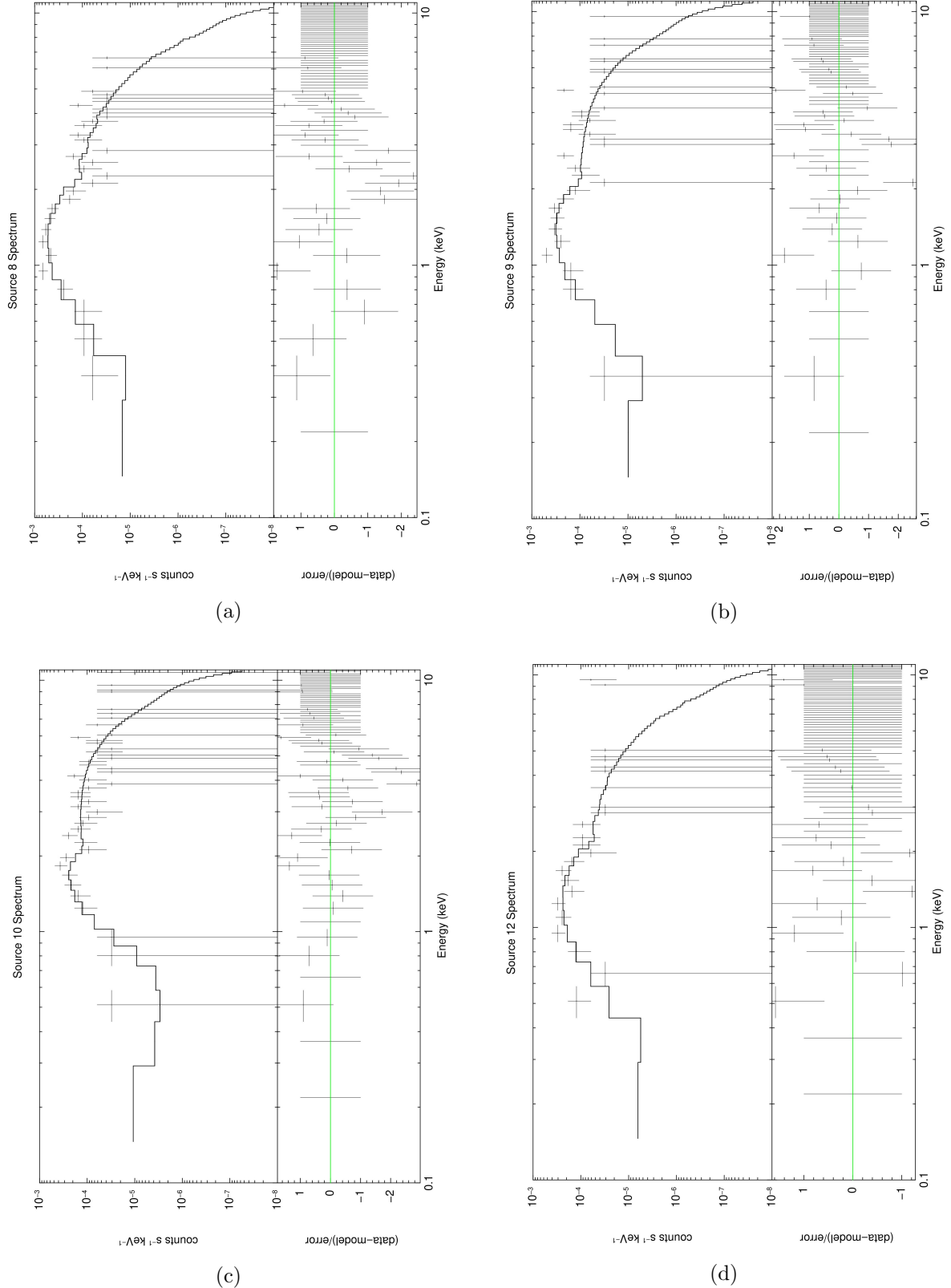


FIG. 5

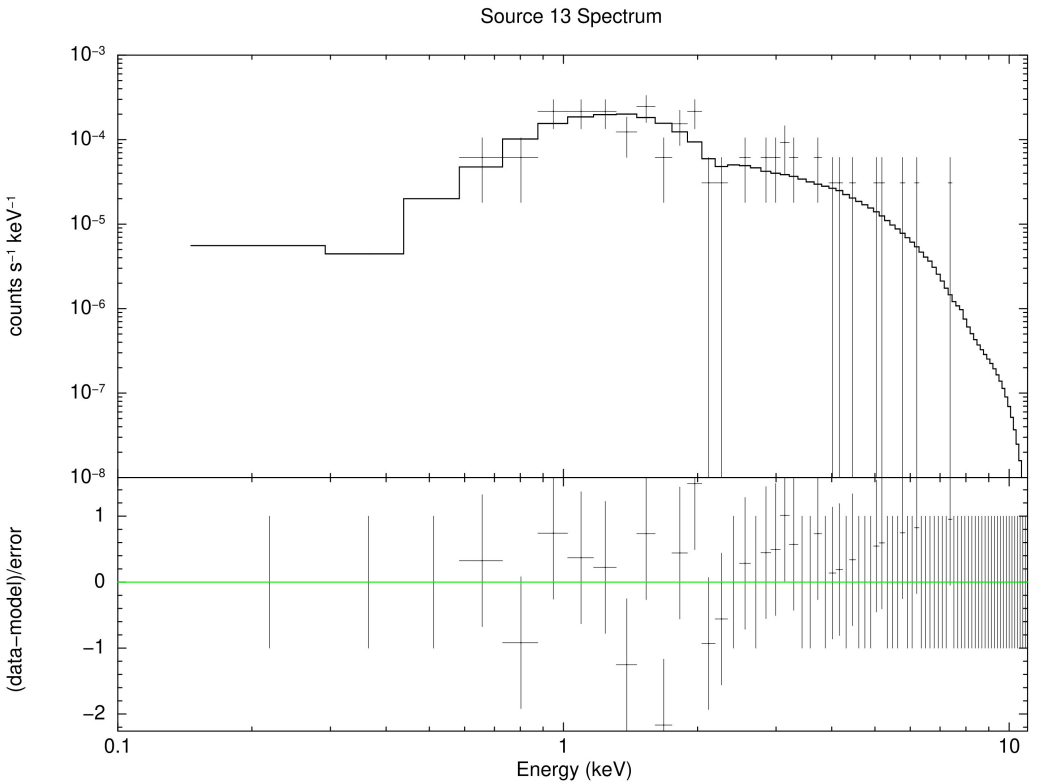


FIG. 6

Appendix B: Script for automated parameter estimation and plotting

```

statistic cstat
method leven 1000 0.01
abund lpgr
xsect vern
cosmo 70 0 0.73
xset delta 0.01
systematic

for {set i 1} {$i < 5} {incr i} {
    data [format "comb%d_src.pi" $i]
    ig bad

    query yes
    model TBabs*vmekal
    0.237065      0.001      0.09      0.09      100000
1e+06          10         0.01      0.0808      0.0808      79.9
79.9          0.3        -0.01     1e-06     1e-05      1e+19
1e+20

```

```

1000          1      -0.01      0      0      1000
1000          1      -0.01      0      0      1000
1000          1      -0.01      0      0      1000
1000          1      -0.01      0      0      1000
1000          1      -0.01      0      0      1000
1000          1      -0.01      0      0      1000
1000          1      -0.01      0      0      1000
1000          1      -0.01      0      0      1000
1000          1      -0.01      0      0      1000
1000          1      -0.01      0      0      1000
1000          1      -0.01      0      0      1000
1000          1      -0.01      0      0      1000
1000          1      -0.01      0      0      1000
1000          1      -0.01      0      0      1000
1000          1      -0.01      0      0      1000
1000          1      -0.01      0      0      1000
1000          1      -0.01      0      0      1000
1000          1      -0.01      0      0      1000
1000          1      -0.01      0      0      1000
1000          1      -0.01      0      0      1000
1000          0.03    -0.01      0      0      1000
1000          1      -0.01      0      0      1000
1000          1      -0.01      0      0      1000
1000          1      -0.01      0      0      1000
1000          0      -0.01    -0.999   -0.999     10
10
           2
0.000111271    0.01      0      0      1e+20
1e+24
 bayes off

renorm
fit 10

if {$i != 4} {
  error 1 2 20
# writefits [format "src-%d-spectrum.fits" $i]
tclout error 1
set err1 $xspec_tclout
tclout error 2
set err2 $xspec_tclout
tclout error 20
set err20 $xspec_tclout

```

```

set err [list $err1 $err2 $err20]
set fp [open [format "src-%d-error.txt" $i] , w+]
puts $fp $err
close $fp
} elseif {$i == 10} {
    error 1 20
# writefits [format "src-%d-spectrum.fits" $i]
tclout error 1
set err1 $xspec_tclout
tclout error 2
set err2 $xspec_tclout
tclout error 20
set err20 $xspec_tclout
set err [list $err1 $err2 $err20]
set fp [open [format "src-%d-error.txt" $i] , w+]
puts $fp $err
close $fp
}

lumin 0.5 6 1.2e-6 err 20,90
tclout lumin
set lum $xspec_tclout
set fp [open [format "src-%d-lumin.txt" $i] , w+]
puts $fp $lum
close $fp

setplot en
setplot rebin 10, 15

#init plotting and save model
save all [format "src-%d-spectrum.xcm" $i]
cpd [format "src-%d-spectrum.ps" $i]/cps

# set the plot formatting
setplot co label top [format "Source-%d-Spectrum" $i]
setplot co rescale y 1.e-6 5e-2
setplot co rescale x 0.1 11
setplot co time off

# plot log-log and residuals
plot ld del
cpd none
}

for {set i 5} {$i < 12} {incr i} {
    data [format "comb%d_src.pi" $i]
    ig bad
}

```

```

query yes
model TBabs*vmekal
      0.237065      0.001      0.09      0.09      100000
1e+06          10      0.01      0.0808      0.0808      79.9
79.9          0.3     -0.01    1e-06    1e-05      1e+19
1e+20          1     -0.01      0      0      1000
1000          1     -0.01      0      0      1000
1000          1     -0.01      0      0      1000
1000          1     -0.01      0      0      1000
1000          1     -0.01      0      0      1000
1000          1     -0.01      0      0      1000
1000          1     -0.01      0      0      1000
1000          1     -0.01      0      0      1000
1000          1     -0.01      0      0      1000
1000          1     -0.01      0      0      1000
1000          1     -0.01      0      0      1000
1000          1     -0.01      0      0      1000
1000          1     -0.01      0      0      1000
1000          1     -0.01      0      0      1000
1000          1     -0.01      0      0      1000
1000          1     -0.01      0      0      1000
1000          1     -0.01      0      0      1000
1000          1     -0.01      0      0      1000
1000          1     -0.01      0      0      1000
1000          0.03     -0.01      0      0      1000
1000          1     -0.01      0      0      1000
1000          0     -0.01    -0.999    -0.999      10
10          2
0.000111271      0.01      0      0      0      1e+20
1e+24
bayes off

renorm
fit 10

```

```

if {$i != 10 && $i !=8} {
  error 1 2 20
  # writefits [format "src-%d-spectrum.fits" $i]
  tclout error 1
  set err1 $xspec_tclout
  tclout error 2
  set err2 $xspec_tclout
  tclout error 20
  set err20 $xspec_tclout
  set err [list $err1 $err2 $err20]
  set fp [open [format "src-%d-error.txt" $i], w+]
  puts $fp $err
  close $fp
} elseif {$i == 8} {
  error 2 20
  # writefits [format "src-%d-spectrum.fits" $i]
  tclout error 1
  set err1 $xspec_tclout
  tclout error 2
  set err2 $xspec_tclout
  tclout error 20
  set err20 $xspec_tclout
  set err [list $err1 $err2 $err20]
  set fp [open [format "src-%d-error.txt" $i], w+]
  puts $fp $err
  close $fp
} elseif {$i == 10} {
  error 1 20
  # writefits [format "src-%d-spectrum.fits" $i]
  tclout error 1
  set err1 $xspec_tclout
  tclout error 2
  set err2 $xspec_tclout
  tclout error 20
  set err20 $xspec_tclout
  set err [list $err1 $err2 $err20]
  set fp [open [format "src-%d-error.txt" $i], w+]
  puts $fp $err
  close $fp
}
lumin 0.5 6 1.2e-6 err 20,90
tclout lumin
set lum $xspec_tclout
set fp [open [format "src-%d-lumin.txt" $i], w+]
puts $fp $lum
close $fp

```

```

setplot en
setplot rebin 8, 10

#init plotting and save model
save all [format "src-%d-spectrum.xcm" $i]
cpd [format "src-%d-spectrum.ps" $i]/cps

# set the plot formatting
setplot co label top [format "Source-%d-Spectrum" $i]
setplot co rescale y 1.e-8 1e-3
setplot co rescale x 0.1 11
setplot co time off

# plot log-log and residuals
plot ld del
cpd none
}

for {set i 12} {$i < 14} {incr i} {
    data [format "comb%d_src.pi" $i]
    ig bad

    query on
    model TBabs*vmekal
        1      0.001      0.09      0.09      100000
1e+06
        10     0.01      0.0808      0.0808      79.9
79.9
        0.3    -0.01      1e-06      1e-05      1e+19
1e+20
        1     -0.01      0          0          1000
1000
        1     -0.01      0          0          1000
1000
        1     -0.01      0          0          1000
1000
        1     -0.01      0          0          1000
1000
        1     -0.01      0          0          1000
1000
        1     -0.01      0          0          1000
1000
        1     -0.01      0          0          1000
1000
        1     -0.01      0          0          1000
1000

```

```

1000          1      -0.01        0        0      1000
1000          1      -0.01        0        0      1000
1000          1      -0.01        0        0      1000
1000          1      -0.01        0        0      1000
1000          1      -0.01        0        0      1000
1000          0.03     -0.01        0        0      1000
1000          1      -0.01        0        0      1000
1000          0      -0.01     -0.999    -0.999      10
10           2
1e+24  0.000111271      0.01        0        0      1e+20
bayes off

# conform the fit to the specific data set
newpar 1 0.09
freeze 1

renorm
fit 10

error 1 2 20
# writefits [format "src-%d-spectrum.fits" $i]
tclout error 1
set err1 $xspec_tclout
tclout error 2
set err2 $xspec_tclout
tclout error 20
set err20 $xspec_tclout
set err [list $err1 $err2 $err20]
set fp [open [format "src-%d-error.txt" $i], w+]
puts $fp $err
close $fp

lumin 0.5 6 1.2e-6 err 20,90
tclout lumin
set lum $xspec_tclout
set fp [open [format "src-%d-lumin.txt" $i], w+]
puts $fp $lum
close $fp

setplot en

```

```
setplot rebin 6, 10

#init plotting and save model
save all [format "src-%d-spectrum.xcm" $i]
cpd [format "src-%d-spectrum.ps" $i]/cps

# set the plot formatting
setplot co label top [format "Source-%d-Spectrum" $i]
setplot co rescale y 1.e-8 1e-3
setplot co rescale x 0.1 11
setplot co time off

# plot log-log and residuals
plot ld del
cpd none
}
```